



Green Synthesis of Silver Nanoparticles Using Marine Fungus *Cladosporium herbarum*: An Assessment of their Antimicrobial Activity

Manar A. Basheer^{1*}, Nermine N. Abed², Khaled Abutaleb^{1,3,4}, Amal A. Mekawey⁵

1 National Authority for Remote Sensing and Space Sciences (NARSS), 23 Joseph Tito Street, El-Nozha El-Gedida, Cairo 1564, Egypt

2 Faculty of Science (Girls Branch), Al-Azhar University Egypt, Nasr City, Cairo 11884, Egypt

3 Agricultural Research Council, Natural Resources and Engineering (ARC-NRE), Pretoria, South Africa

4 School of Animal, Plant and Environmental Sciences, University of Witwatersrand, Private Bag X3, Johannesburg, 2050, South Africa

5 The Regional Center of Mycology and Biotechnology, Al-Azhar University, Cairo 4434010, Egypt

*Corresponding Author: mmanar2015@gmail.com

ARTICLE INFO

Article History:

Received: Aug. 30, 2023

Accepted: Oct. 4, 2023

Online: Oct. 13, 2023

Keywords:

Silver nanoparticle,
Cladosporium herbarum,
SEM,
TEM,
Antimicrobial activity,
Qarun Lake

ABSTRACT

Green, eco-friendly, cost-effective, safe, and reliable processes for synthesizing nanoparticles using microorganisms as bio-nanofactories have garnered significant interest due to their ability to transform metals into nanoscale particles for use in various fields. In this study, silver nitrate and supernatants from *Cladosporium herbarum*, isolated from water samples of Qarun Lake in Egypt, were utilized for the extracellular biosynthesis of silver nanoparticles (AgNPs), and their effectiveness against various pathogenic microorganisms was assessed. Silver nanoparticles were synthesized using four isolated marine fungi, with optimization of reaction parameters, and the resultant nanoparticles were characterized using a range of analytical techniques including Transmission Electron Microscopy (TEM), Fourier transform infrared (FT-IR), and X-ray analysis. The antimicrobial activity of the biosynthesized silver nanoparticles was evaluated against a variety of pathogens, including both Gram-positive and Gram-negative bacteria, yeast, and fungi. The results demonstrated that silver nanoparticles synthesized by *Cladosporium herbarum* exhibited potent antimicrobial activity against different pathogens under optimal conditions, including a substrate concentration of 5 mM, an incubation temperature of 37°C, a pH value of 6, and a 24-hour incubation period. TEM analysis revealed the formation of spherical, well-dispersed nanoparticles with sizes ranging from 4 to 23.1 nm, while FT-IR spectroscopy indicated prominent absorption bands at 556, 762, 1349, 1451, 1562, 1620, and 3352 cm⁻¹, corresponding to the stretching vibrations of alkyl halides, C-H groups, phenolic O-H groups, amide C-N groups, NH₂ groups, N-H groups, and hydroxyl (OH) groups, respectively. The biosynthesis of silver nanoparticles mediated by *Cladosporium herbarum* holds promise as a potential antimicrobial agent against various pathogenic microbes.

INTRODUCTION

Marine fungi have been shown to contain various bioactive secondary metabolites with unique structures. These bioactive compounds exhibit antibacterial activity against several pathogenic bacteria (**Basheer *et al.*, 2018; Karthikeyan *et al.*, 2022; Arrieche *et al.*, 2023**).

The study by **Wulandari *et al.* (2021)** demonstrated the antimicrobial activities of *Cladosporium* sp. against *Staphylococcus aureus*, *Staphylococcus epidermidis*, *Klebsiella pneumoniae*, *Escherichia coli*, *Bacillus subtilis*, *Bacillus megaterium*, and *Bacillus stearothermophilus*. It also highlighted *Cladosporium* species as a valuable source of pharmaceutical-grade antimicrobial compounds.

Kalyani *et al.* (2017) concluded that marine fungi isolated from the Bay of Bengal in Kakinada exhibited antibacterial activity against a variety of Gram-positive and Gram-negative bacteria.

Marine fungi excrete hydrolytic enzymes that degrade different substances, contributing to the purification of aquatic environments (**Ortiz-Vera *et al.*, 2018**). These fungi represent a unique ecological category, distinct in both morphology and physiological requirements from their terrestrial counterparts. Lakes and ponds provide suitable environments for fungal growth (**El-Sahrouny *et al.*, 2009**). The ecology and growth of marine fungi are influenced by various factors, including habitat, available substrata, geographical distribution, temperature, salinity, competition, organic nutrients, oxygen availability, contaminants, and even light (**Jones, 2000**).

Zhou *et al.* (2016) confirmed that marine fungi isolated from different habitats exhibit varying biological activities, with 142 fungal species from 84 genera displaying 137 distinct types of biological activity.

Marine fungi can be employed for the eco-friendly and cost-effective remediation of contaminants through bioremediation. Bioremediation relies on fungi's ability to eliminate or transform pollutants into harmless products (**Dell'Anno *et al.*, 2021**). Given the potential long treatment periods required for high concentrations of contaminants, the combination of nanomaterials and bioremediation holds promise (**Cecchin *et al.*, 2017**). Nanotechnology can significantly enhance pollutant remediation efficiency when integrated with conventional treatment methods (**Mobasser & Firoozi, 2016**).

Biosynthesis of nanomaterials offers advantages over chemical methods, as it employs non-toxic agents and results in higher efficiency, reducing health and environmental concerns (**Dorcheh & Vahabi, 2016**). Nanomaterials enhance microbial activity against

specific waste and toxic substances, reducing time and cost (**Rizwan *et al.*, 2014;** **Darwesh *et al.*, 2022**).

Moustafa's study (2017) emphasized the efficiency of biological techniques in nanomaterial synthesis compared to traditional chemical and physical methods. Fungi, in particular, are favored for metal nanoparticle synthesis due to their ability to secrete large quantities of enzymes and proteins. Handling fungal biomass in the laboratory is straightforward and cost-effective. For example, *Aspergillus flavus* demonstrated the ability to synthesize extracellular AgNPs with high antibacterial activity, achieving one hundred percent removal efficiency against faecal coliform. Additionally, biosynthesized nanomaterials have shown promise as antimicrobial agents against various pathogens causing waterborne disease.

Popli *et al.* (2018) revealed that extracts of *Cladosporium* sp. contain biomolecules responsible for reducing and capping biosynthesized silver nanoparticles.

Qarun Lake is one of the Egyptian lakes suffering from low water quality due to bacterial contaminants (**Abdelmageed *et al.*, 2022**). This study aimed to biosynthesize silver nanoparticles using marine fungi isolated from Qarun Lake and assess the antibacterial activity of the biosynthesized nanoparticles. These nanoparticles may subsequently find application in the treatment or nano-bioremediation of microbial contaminants in Qarun Lake ultimately improving water quality.

MATERIALS AND METHODS

Isolation and identification of fungi for silver nanoparticle synthesis

Fifteen water samples were collected from Qarun Lake, Egypt, and stored in sterile containers at 4°C. The growth and preservation of fungal cultures were conducted using Malt Extract Agar (MEA) medium. Fungal identification took place at the Regional Center for Mycology and Biotechnology (RCMB), Al-Azhar University based on morphological and reproductive characteristics. Ten different isolates belonging to five species were identified, with one particular fungus predominating. This predominant fungus was cultured in Malt Extract Broth (MEB) at 28°C on a rotary shaker (120 rpm) for 7 days. Subsequently, the biomass was harvested via filtration and washed with distilled water. Approximately, 20g of wet biomass was mixed with 100mL of distilled water and incubated at 28°C for 24 hours on a rotary shaker. Following incubation, the biomass was filtered, and the resulting cell filtrate was collected for the biosynthesis of AgNPs, following the method outlined by **Devi and Joshi (2012)**. For the extracellular biosynthesis of AgNPs, a solution of silver nitrate (AgNO₃) was added to yield various

concentrations of silver ions, ranging from 1 to 10mM. The mixture was incubated at 28°C for 7 days in the dark to prevent any photochemical reactions until a noticeable change in color occurred.

Optimization of reaction parameters for the biosynthesis of AgNPs

Various parameters were optimized by systematically changing them one at a time. To determine the optimal incubation time and wavelength for the biosynthesis of AgNPs, a mixture comprising 20mL of 1mM AgNO₃ and 20mL of cell filtrate was agitated in the dark at pH 7 and a temperature of 37°C. Optical density measurements were taken at various time intervals. AgNO₃ concentrations ranging from 1 to 10mM were added to the fungal filtrate, followed by incubation at temperatures of 15, 20, 28, 37, and 50°C, as well as pH levels of 5, 6, 7, 8, 9, and 10 for substrate concentration, temperature, and pH optimization, respectively. The optical absorbance was recorded at different time intervals using the optimal wavelength. Absorption spectra were measured within the range of 200 to 800nm, and the optimal incubation time was determined at different intervals.

Characterization of AgNPs

Several techniques were employed to characterize the silver nanoparticles, including visual observation, UV-Visible spectroscopy, energy-dispersive X-ray (EDX) analysis in conjunction with Scanning Electron Microscopy (SEM), X-ray diffraction (XRD) analysis using Transmission Electron Microscopy (TEM), TEM and Fourier transform infrared (FT-IR) analysis.

UV-visible spectroscopy analysis

The reduction of silver ions was verified using UV-visible spectrophotometer (Milton-Roy Spectronic 1201 UV) after 48 hours. The absorption spectra of the supernatants were taken between 200 and 800nm.

TEM analysis

The diameter, size, and shape of AgNPs were determined using TEM (JEOL 1010 TEM, Japan). The sample was prepared by placing a solution drop containing the biosynthesized AgNPs onto a TEM grid made of carbon-coated copper with 400 meshes (PlanoGmbH, Germany). Electron micrographs of the sample were captured using an accelerating voltage of 80 kV at the Regional Center for Mycology and Biotechnology.

SEM analysis

EDX spectra (SEM/EDX, JSM.550 LV [JEOL, SEM, Japan]) were used for morphology analysis. Surface binding elements were analyzed with X-ray photoelectron spectroscopy and showed peak values of Ag element.

FT-IR spectroscopy analysis

A FT-IR spectrometer (IRPrestige-21®, German) was used to analyze the interaction between proteins and nanoparticles, as well as to detect biomolecules involved in the reduction of Ag⁺ ions, following the standard operating protocol. The fungal filtrate, which contained nanoparticles, was subjected to agitation at 5000rpm for 10 minutes, followed by washing with deionized water and air-drying. FT-IR spectra were recorded within the range of 450 - 4000 cm⁻¹ at a resolution of 4 cm⁻¹.

Antimicrobial activity of the biosynthesized AgNPs

The antimicrobial activity of synthesized AgNPs was investigated against eight species of pathogenic bacteria: *Escherichia coli*, *Klebsiella pneumoniae*, *Proteus vulgaris*, *Salmonella typhi* (Gram-negative bacteria), *Enterococcus faecalis*, Methicillin-Resistant *Staphylococcus aureus* (MRSA), *Staphylococcus hominis*, and *Staphylococcus epidermidis* (Gram-positive bacteria); two species of pathogenic yeast (*Candida albicans*, *Candida tropicalis*); and three species of pathogenic fungi (*Aspergillus niger*, *Penicillium expansum*, *Rhizopus oryzae*) using the agar well diffusion method. All pathogens were obtained from the antimicrobial unit at RCMB, Al-Azhar University. The overnight-grown bacteria and yeast cultures were plated on Nutrient Agar media, while fungal cultures were plated on Malt Extract agar media. Wells with a diameter of 6mm were cut, and 50µL of AgNPs solution at each concentration were added to each well. The cell filtrate alone was used as a control. One well was filled with chloramphenicol or griseofulvin as positive control. The plates were refrigerated for 30 minutes and then incubated overnight at 37°C for bacteria and yeast and at 28°C for fungi. The plates were subsequently observed for the presence of zones of inhibition after 24-48 hours of incubation.

Minimal inhibitory concentration (MIC) of AgNPs

The broth microdilution technique was employed to determine the MIC values. Approximately, 10µL of each bacterial culture was introduced into 10mL of nutrient broth, followed by treatment with varying concentrations of AgNPs, ranging from 30 to 10 µg/mL. These mixtures were subsequently incubated at 37°C for 24 hours, while the control group solely consisted of broth. The MIC was the minimum AgNPs concentration that ceases the bacterial growth (Abed & Mohammed, 2021). Visual turbidity in the tubes was observed to confirm the MIC value.

Effect of AgNPs on microbial morphology and ultrastructure

The morphological and ultrastructural alterations induced by AgNPs in the most sensitive tested microorganisms (*C. tropicalis* and *S. hominis*) were analyzed by TEM at RCMB using a voltage of 70 kV following treatment with their respective MICs of AgNPs (25µg/mL for *C. tropicalis* and 30µg/mL for *S. hominis*).

RESULTS

Isolation and identification of marine fungi

Table (1) and Fig. (1) display the macroscopic and microscopic characteristics of the predominant fungus. Its colonies are characterized by colors ranging from olivaceous green to olivaceous brown, with an olivaceous black reverse. Microscopic examination revealed smooth-walled conidiophores with a color ranging from pale to olivaceous green, as well as ellipsoidal to cylindrical conidia with smoothly rounded ends, all of which were identified as belonging to *Cladosporium herbarum*.

Table1. Macroscopic and microscopic characteristics of *Cladosporium herbarum*

Isolate	Macroscopic characteristics		Microscopic characteristics	
	Surface color	Reverse	Conidiophore	Conidia Phialides
<i>Cladosporium herbarum</i>	Olivaceous green (Papazlatani <i>et al.</i> 2022)	Greenish black	Smooth, hyaline	Ellipsoidal to cylindrical, 5.5-13.0 x 3.8-6.0 μm

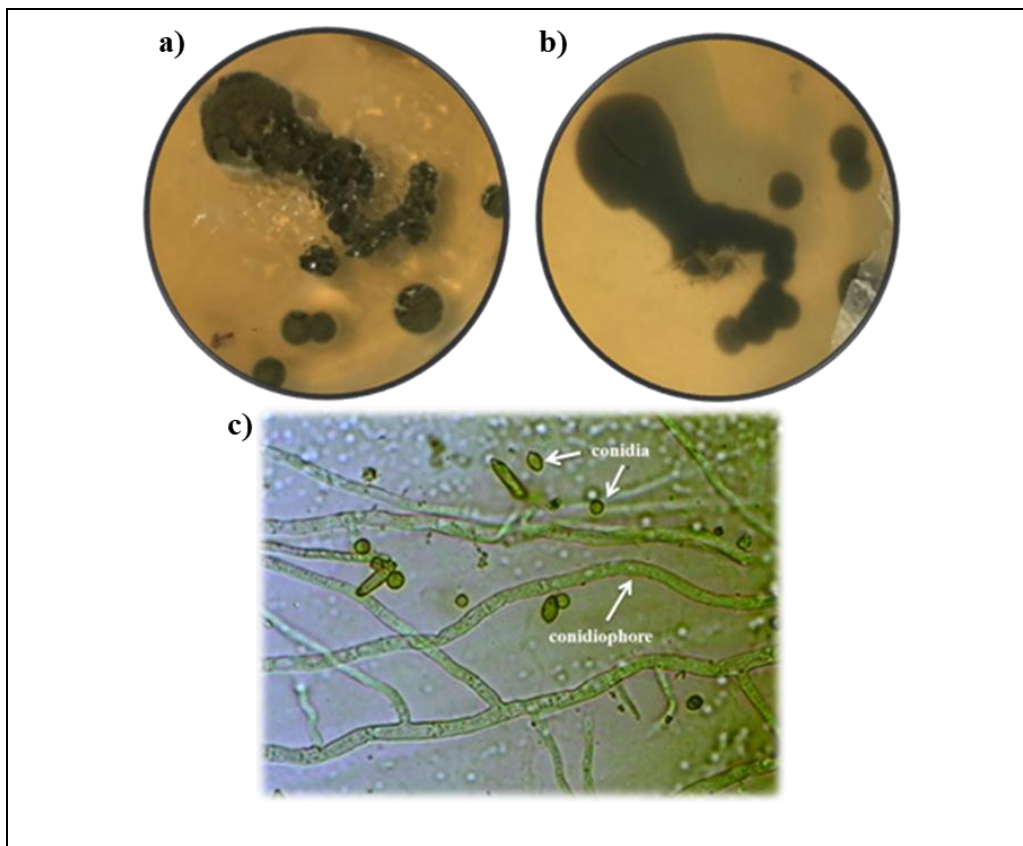


Fig. 1. *Cladosporium herbarum* (a) Colony on MEA; (b) Colony reverse; (c) Microscopic characteristics

Optimization result of reaction parameters for the biosynthesis of AgNPs

The cell filtrate, when incubated with AgNO_3 solution in the dark, exhibited a gradual change in the medium's color, transitioning to brown, with the intensity increasing over time. This color change, indicative of silver nanoparticle synthesis, was visually observed. In contrast, the control (without AgNO_3) displayed no color change when subjected to the same conditions.

The results indicated an increased absorption intensity between 400 and 500nm. Consequently, optical density measurements were taken at equal time intervals to precisely identify the optimum wavelength. The results revealed a peak at 430nm as the optimal ultraviolet wavelength for measuring AgNPs in all filtrates.

Fig. (3) illustrates the ideal incubation time, optimal silver nitrate concentration, temperature, and pH. Furthermore, the results indicated that three concentrations (2, 5, and 8 mM) exhibited the highest absorbance.

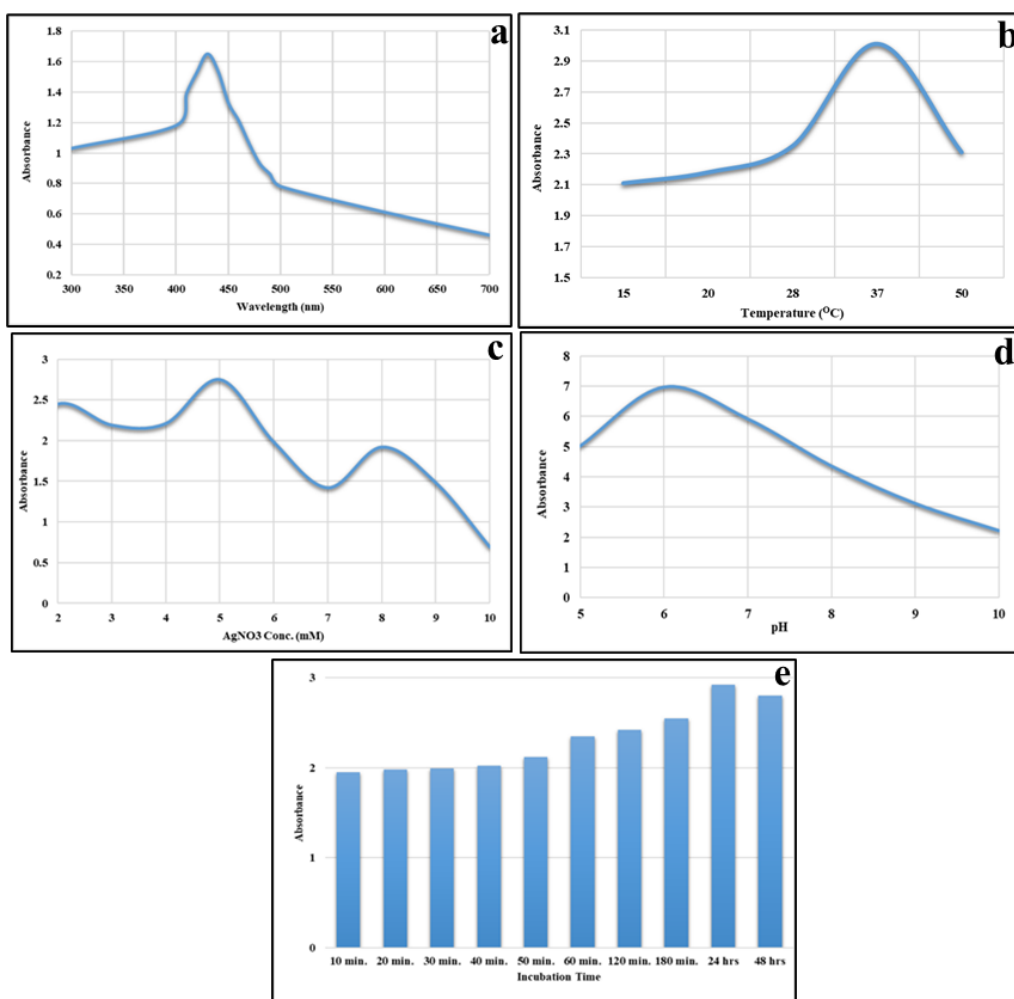


Fig. 2. UV-Vis spectrum for optimization studies of AgNPs production at (a) different wavelength, (b) different temperature, (c) different silver nitrate concentration, (d) different pH and (e) different incubation time

TEM analysis of AgNPs

The high-resolution TEM images provided clarity on the nanoparticles characteristics, confirming their high stability, small size, monodispersity, and spherical shape. The particle sizes ranged from 4 to 23.1nm (Fig. 3).

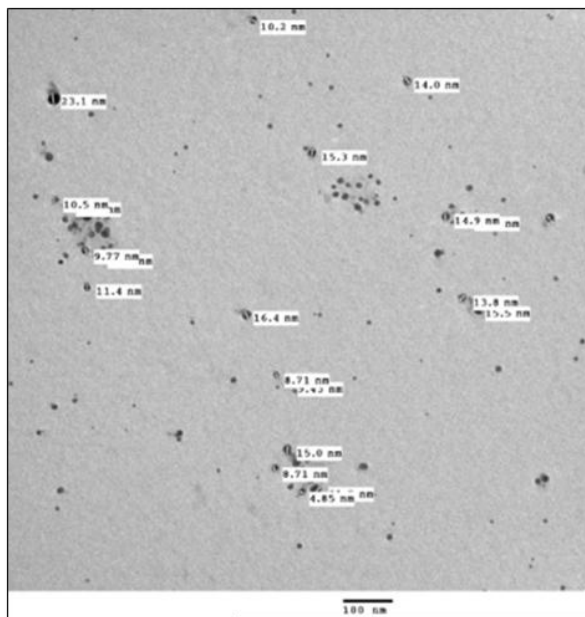


Fig. 3. TEM micrograph of synthesized AgNPs (Scale bar: 100nm) mediated by *C. herbarum*

Energy dispersive X-ray / SEM analysis

The presence of elemental silver was proven by EDX analysis. The optical absorption peak is observed approximately at 3 keV (Fig. 4).

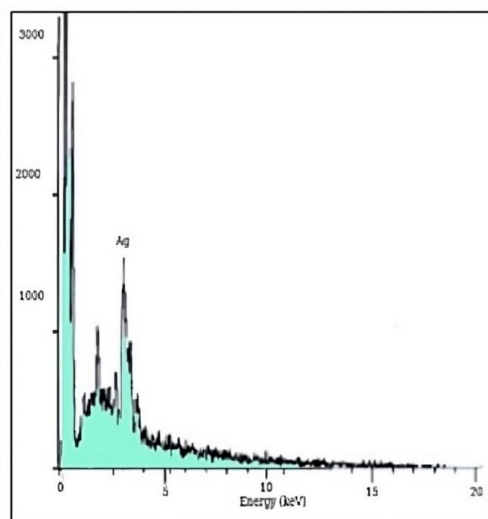


Fig. 4. EDX spectrum of the biosynthesized AgNPs

X-ray diffraction analysis result

XRD patterns (Fig. 5) confirmed the crystalline nature of the biosynthesized silver nanoparticle by showing intense peaks ranging from 20° to 80° . The XRD spectrum measuring the fungal extracts resulted in four intense peaks.

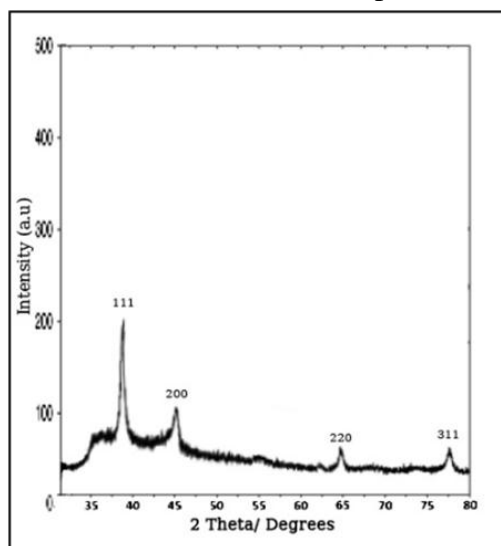


Fig. 5. XRD patterns of the biosynthesized AgNPs

FT-IR result

FT-IR analyses produce an infrared absorption spectrum for identifying the types of chemical bonds in a molecule, which are considered a "fingerprint". FT-IR spectra of the biosynthesized nanoparticles exhibited absorption peaks at 556, 762, 1349, 1451, 1562, 1620, and 3350 cm^{-1} , revealing the presence of various functional groups (Fig. 6).

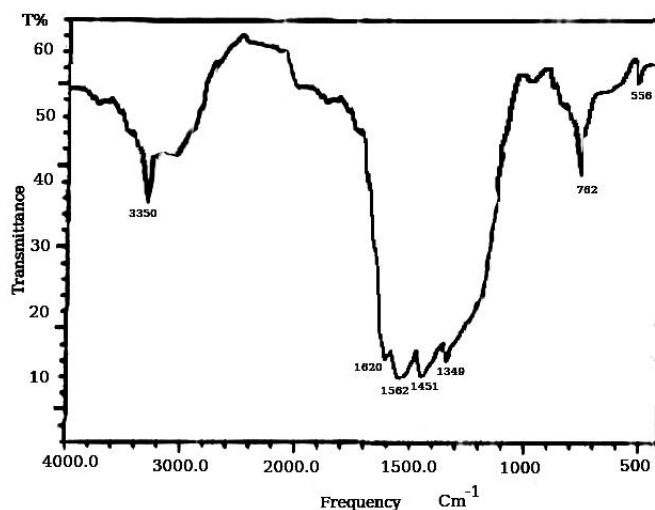


Fig. 6. FT-IR spectra of the biosynthesized AgNPs mediated by *C. herbarum*

Antimicrobial activity

AgNPs at the most effective concentrations (2, 5, and 8 mM), which exhibited higher zones of inhibition, were employed in the antimicrobial activity tests against the tested microorganisms. The diameters of the inhibition zones were measured in millimeters. AgNPs displayed activity against all the tested bacterial pathogens, except for MRSA, as well as against all the tested pathogenic yeasts and fungi, except for *A. niger* (Tables 2, 3). Among the microorganisms, *S. hominis* and *C. tropicalis* exhibited the highest sensitivity as shown in Fig. (7).

Table 2. Antibacterial activity of the myco-biosynthesized AgNPs

Antibacterial activity (mm)			
	2 mM	5 mM	8 mM
<i>Enterococcus faecalis</i>	13±2	15±1	15±0
<i>Escherichia coli</i>	15±1	14±0	13±0
<i>Klebsiella pneumoniae</i>	Null	15±1	18±1
<i>Methicillin-resistant Staphylococcus aureus</i>	Null	Null	Null
<i>Proteus vulgaris</i>	21±2	25±2	20±0
<i>Salmonella typhi</i>	15±2	25±1	21±0
<i>Staphylococcus hominis</i>	26±1	20±2	22±2
<i>Staphylococcus epidermidis</i>	12±1	14±0	16±2
Null: no activity			

Table 3. Antifungal activity of the myco-biosynthesized AgNPs

Antifungal activity (mm)			
	2 mM	5 mM	8 mM
<i>Candida albicans</i>	Null	11±0	10±2
<i>Candida tropicalis</i>	12±2	14±2	11±2
<i>Aspergillus niger</i>	Null	Null	Null
<i>Rhizopus oryzae</i>	12±2	13±1	10±0
<i>Penicillium expansum</i>	11±2	11±1	14±0
Null: no activity			

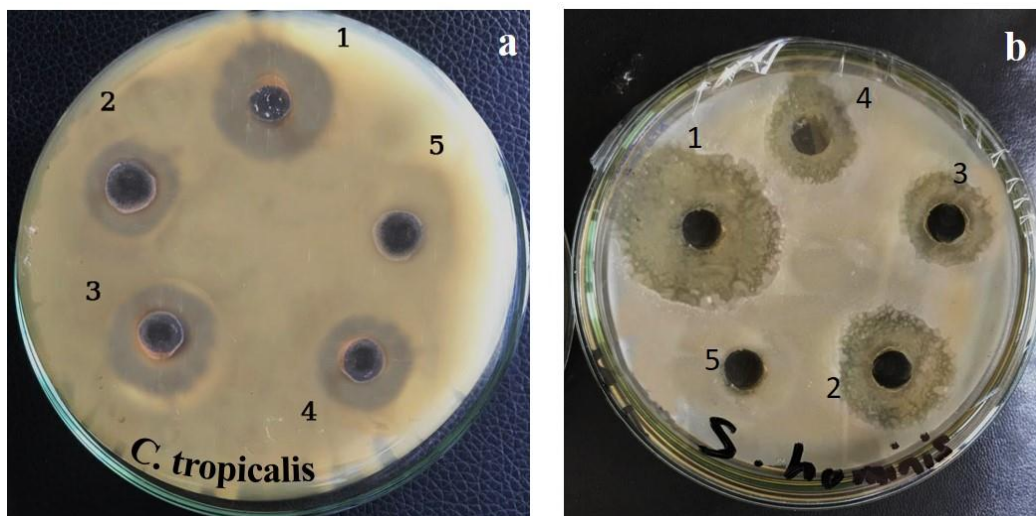


Fig. 7. Antimicrobial activity against **a)** *C. tropicalis* and **b)** *S. hominis* (1: Chloramphenicol or griseofulvin, 2: 2 mM, 3: 5 mM, 4: 8 mM 5: Control)

Effect of AgNPs on microbial morphology and ultrastructure

C. tropicalis cells exhibited significant alterations in their cell wall and cell membrane when compared to intact cells (Fig. 8). TEM analysis revealed the attachment and accumulation of AgNPs on the cell wall and cell membranes, as well as their penetration into the cells. This accumulation in the cytoplasm resulted in the bursting of the cell wall and the degeneration of the cytoplasmic membrane, leading to substantial intracellular damage. Additionally, TEM analysis indicated that the cell walls of *C. tropicalis* appeared shrunken and collapsed. Morphological and ultrastructural changes were also observed in *S. hominis* cells, as shown in Fig. (9).

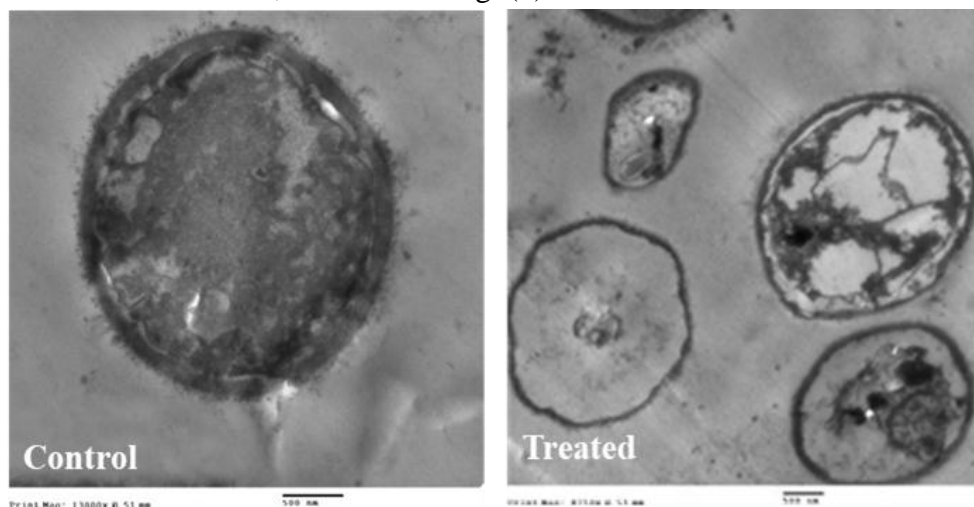


Fig. 8. Ultrastructure alteration in *C. tropicalis* after treatment with the MIC of AgNPs

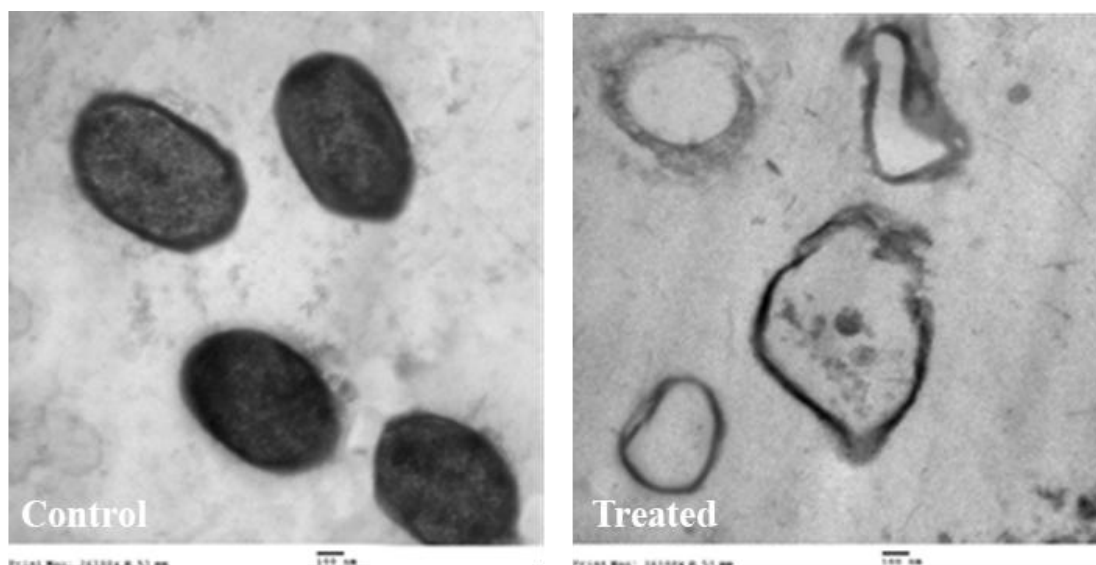


Fig. 9. Ultrastructure alteration in *S. hominis* after treatment with the MIC of AgNPs

DISCUSSION

The synthesis of nanoparticles (NPs) mediated by fungi offers several advantages over traditional NP synthesis methods. One significant advantage is the ability to optimize NP properties by making slight adjustments to reaction parameters. This approach has the potential to become a pivotal technology in the future due to the high surface-to-volume ratio of the resulting NPs and their dual functionality as both antibacterial agents and bioactive fungal capping agents.

The appearance of a brown color during the optimization of reaction parameters for AgNPs biosynthesis served as a clear indicator of colloidal silver particle formation in the medium (Lotfy *et al.*, 2021; Mohamed *et al.*, 2022). The increase in color intensity likely results from the rising number of synthesized nanoparticles due to the reduction of silver ions present in the aqueous solution.

TEM analysis results unveiled that the small size of the AgNPs plays a critical role in their antimicrobial activity. Consequently, antimicrobial activity increases as the size of the NPs decreases (Femi-Adepoju *et al.*, 2019).

XRD-spectrum analysis of fungal extracts produced four intense peaks, corresponding to Bragg's reflections of silver nanocrystals (Lu *et al.*, 2003; Maduraimuthu *et al.*, 2023). These results align with Shaligram *et al.* (2009) study, confirming that the silver nanoparticles exist in the form of silver nanocrystals, as indicated by the X-ray diffraction pattern and their crystalline structure.

FT-IR absorption peaks at 556, 762, 1349, 1451, 1562, 1620, and 3350 cm^{-1} signify the presence of specific chemical groups: NH_2 group (Panwar *et al.*, 2015), C-N group of amide (Salaheldin *et al.*, 2017), stretching of alkyl halides (Kalaivani *et al.*, 2018),

stretching vibration of –OH group (Rahman *et al.*, 2022), C-H group, O-H group of phenol (Suriyakala *et al.*, 2022), and N-H group (Wahab *et al.*, 2022).

The effectiveness of AgNPs on the morphological features and ultrastructure of *C. tropicalis* can be explained via referring to the studies conducted by Kim *et al.* (2009) and Jalal *et al.* (2019). These studies suggest that the anticandidal mechanisms of AgNPs may involve the formation of holes in the cell wall and cell membrane, leading to cell damage and, ultimately, cell death. In the case of *S. hominis*, the small size of the synthesized AgNPs may enhance their penetration of the cell, resulting in the loss of cell viability and antimicrobial activity by disrupting cell membrane integrity. In addition, the morphological and ultrastructural findings are consistent with the results reported by Wady *et al.* (2014).

Antimicrobial activity results align with More *et al.* (2023) study, which revealed that silver nanoparticles continuously release silver ions, potentially causing microorganism destruction. Silver ions are attracted to sulfur proteins electrostatically, allowing them to adhere easily to cell walls and cytoplasmic membranes. This adherence enhances cell permeability, leading to cell breakdown and the disruption of the bacterial envelope.

CONCLUSION

The synthesis of AgNPs was facilitated by the extract of marine fungus *Cladosporium herbarum*, which acted as a potential stabilizing and reducing agent. Various characterization techniques, including FT-IR, SEM, EDX, TEM, and XRD were employed to analyze the resulting AgNPs. FT-IR spectroscopy confirmed the presence of functional biomolecules. SEM supported TEM findings, revealing a spherical morphology for the AgNPs. The size of the AgNPs was estimated to range from 4 to 23.1 nm. EDX analysis validated the elemental composition of AgNPs, with a prominent signal at 3.0 keV corresponding to silver. XRD analysis demonstrated the crystallinity of the AgNPs.

The biosynthesized AgNPs exhibited effective antimicrobial activity against the majority of the selected pathogens. Consequently, AgNPs are suggested as valuable products in the field of nanobiotechnology. Understanding the behavior of AgNPs in biological environments equips scientists with the knowledge needed to develop new technologies and nanomaterials for combatting various pathogens.

The results of this study promote the use of green nanoparticles in wastewater treatment procedures in the near future to improve water quality.

REFERENCES

- Abed, K. and Mohammed, A. E.** (2021). Synergistic and antagonistic effects of biogenic silver nanoparticles in combination with antibiotics against some pathogenic microbes. *Frontiers in Bioengineering and Biotechnology*, 9: 652362.
- Abdelmageed, A. A.; Khalifa, U.; Elsaied, H. E.; Hamouda, A. Z. and El Gelani, S. S.** (2022). Lake Qarun between entangled history and blurred future: Retrospectives and prospective. *The Egyptian Journal of Aquatic Research*, 48(4): 299-306.
- Arrieche, D.; Cabrera-Pardo, J. R.; San-Martin, A.; Carrasco, H. and Taborga, L.** (2023). Natural products from Chilean and Antarctic marine fungi and their biomedical relevance. *Marine Drugs*, 21(2),98. <https://doi.org/10.3390/md21020098>.
- Basheer, M. A.; Mekawey, A. A.; El-Kafrawy, S. B. and Abouzeid, M. A.** (2018). Antimicrobial activities of endophytic fungi of Red Sea aquatic plant *Avicennia marina*. *Egyptian Journal of Microbiology*, 53(1): 231-240, doi:10.21608/ejm.2018.3833.1082.
- Cecchin, I.; Reddy, K. R.; Thomé, A.; Tessaro, E. F. and Schnaid, F.** (2017). Nanobioremediation: Integration of nanoparticles and bioremediation for sustainable remediation of chlorinated organic contaminants in soils. *International Biodeterioration and Biodegradation*, 119: 419-428.
- Darwesh, O. M.; Li, H. and Matter, I. A.** (2022). Nano-bioremediation of textile industry wastewater using immobilized CuO-NPs myco-synthesized by a novel Cu-resistant *Fusarium oxysporum* OSF18. *Environmental Science and Pollution Research*, pp.1-13.
- Dell'Anno, F.; Rastelli, E.; Sansone, C.; Brunet, C.; Ianora, A. and Dell'Anno, A.** (2021). Bacteria, fungi and microalgae for the bioremediation of marine sediments contaminated by petroleum hydrocarbons in the omics era. *Microorganisms*, 9(8): 1695. <https://doi.org/10.3390/microorganisms9081695>.
- Dorcheh, S. and Vahabi, K.** (2016). Biosynthesis of nanoparticles by fungi: large-scale production. *Fungal metabolites*. Springer International Publishing, Switzerland, pp. 1-20.
- El-Sharouny, H. M.; Gherbawy, Y. A. and Abdel-Aziz, F. A.** (2009). Fungal diversity in brackish and saline lakes in Egypt. *Nova Hedwigia*, 89(3): 437-450.
- Femi-Adepoju, A. G.; Dada, A. O.; Otun, K. O.; Adepoju, A. O. and Fatoba, O. P.** (2019). Green synthesis of silver nanoparticles using terrestrial fern (*Gleichenia Pectinata* (Willd.) C. Presl.): characterization and antimicrobial studies. *Heliyon*, 5(4). <https://doi.org/10.1016/j.heliyon.2019.e01543>.
- Jalal, M.; Ansari, M. A.; Alzohairy, M. A.; Ali, S. G.; Khan, H. M.; Almatroudi, A. and Siddiqui, M. I.** (2019). Anticandidal activity of biosynthesized silver nanoparticles: effect on growth, cell morphology, and key virulence attributes of *Candida* species. *International Journal of Nanomedicine*, 14: 4667-4679.
- Jones, E. B. G.** (2000). Marine fungi: Some factors influencing biodiversity. *Fungal Diversity*, 4: 53-73.

- Kalaivani, R.; Maruthupandy, M.; Muneeswaran, T.; Beevi, A. H.; Anand, M.; Ramakritinan, C. M. and Kumaraguru, A. K.** (2018). Synthesis of chitosan mediated silver nanoparticles (Ag NPs) for potential antimicrobial applications. *Frontiers in Laboratory Medicine*, 2(1): 30-35.
- Kalyani, P.; Lakshmi, B. K. M. and Hemalatakha, K. P. J.** (2017). Isolation, identification of marine fungi with antibacterial activity. *International Journal of Current Advanced Research*, 6(12): 8085-8091.
- Karthikeyan, A.; Joseph, A. and Nair, B. G.** (2022). Promising bioactive compounds from the marine environment and their potential effects on various diseases. *Journal of Genetic Engineering and Biotechnology*, 20(1): 1-38.
- Kim, K. J.; Sung, W. S.; Suh, B. K.; Moon, S. K.; Choi, J. S.; Kim, J. G. and Lee, D. G.** (2009). Antifungal activity and mode of action of silver nano-particles on *Candida albicans*. *Biometals*, 22(2): 235-242.
- Lotfy, W. A.; Alkersh, B. M.; Sabry, S. A. and Ghozlan, H. A.** (2021). Biosynthesis of silver nanoparticles by *Aspergillus terreus*: characterization, optimization, and biological activities. *Frontiers in bioengineering and biotechnology*, 9: 633468. doi: 10.3389/fbioe.2021.633468.
- Lu, H. W.; Liu, S. H.; Wang, X. L.; Qian, X. F.; Yin, J. and Zhu, Z. K.** (2003). Silver nanocrystals by hyperbranched polyurethane-assisted photochemical reduction of Ag⁺. *Materials Chemistry and Physics*, 81(1): 104-107.
- Maduraimuthu, V.; Ranishree, J. K.; Gopalakrishnan, R. M.; Ayyadurai, B.; Raja, R. and Heese, K.** (2023). Antioxidant activities of photoinduced phycogenic silver nanoparticles and their potential applications. *Antioxidants*, 12(6): 1298. <https://doi.org/10.3390/antiox12061298>.
- Mobasser, S. and Firoozi, A. A.** (2016). Review of nanotechnology applications in science and engineering. *J Civil Eng Urban*, 6(4): 84-93.
- Mohamed, S. O.; El-Naggar, K. and Khalil, M. M.** (2022). Green synthesis of silver nanoparticles using egyptian propolis extract and its antimicrobial activity. *Egyptian Journal of Chemistry*, 65(7): 453-464.
- More, P. R.; Pandit, S.; Filippis, A. D.; Franci, G.; Mijakovic, I. and Galdiero, M.** (2023). Silver nanoparticles: bactericidal and mechanistic approach against drug resistant pathogens. *Microorganisms*, 11(2): 369.
- Moustafa, M. T.** (2017). Removal of pathogenic bacteria from wastewater using silver nanoparticles synthesized by two fungal species. *Water Science*, 31(2): 164-176.
- Ortiz-Vera, M. P.; Olchanheski, L. R.; da Silva, E. G.; de Lima, F. R.; Martinez, L. R. D. P. R.; Sato, M. I. Z. and Araújo, W. L.** (2018). Influence of water quality on diversity and composition of fungal communities in a tropical river. *Scientific reports*, 8(1): 1-9.
- Panwar, K.; Jassal, M. and Agrawal, A. K.** (2015). In situ synthesis of Ag-SiO₂ Janus particles with epoxy functionality for textile applications. *Particuology*, 19: 107-112.

- Papazlatani, C. V.; Kolovou, M.; Gkounou, E. E.; Azis, K.; Mavriou, Z.; Testembasis, S. and Karpouzas, D. G.** (2022). Isolation, characterization and industrial application of a *Cladosporium herbarum* fungal strain able to degrade the fungicide imazalil. *Environmental Pollution*, 301: 119030.
- Popli, D.; Anil, V.; Subramanyam, A. B. MN, N., VR, R.; Rao, S. N. and Govindappa, M.** (2018). Endophyte fungi, *Cladosporium* species-mediated synthesis of silver nanoparticles possessing in vitro antioxidant, anti-diabetic and anti-Alzheimer activity. *Artificial cells, nanomedicine, and biotechnology*, 46(sup1): 676-683.
- Rahman, F.; Majed Patwary, M. A.; Bakar Siddique, M. A.; Bashar, M. S.; Haque, M. A.; Akter, B. and Royhan Uddin, A. K. M.** (2022). Green synthesis of zinc oxide nanoparticles using *Cocos nucifera* leaf extract: characterization, antimicrobial, antioxidant and photocatalytic activity. *Royal Society Open Science*, 9(11), 220858.
- Rizwan, M. D.; Singh, M.; Mitra, C. K. and Morve, R. K.** (2014). Ecofriendly application of nanomaterials: nanobioremediation. *Journal of Nanoparticles*, 2014: 1-7. <https://doi.org/10.1155/2014/431787>.
- Shaligram, N. S.; Bule, M.; Bhambure, R.; Singhal, R. S.; Singh, S. K.; Szakacs, G. and Pandey, A.** (2009). Biosynthesis of silver nanoparticles using aqueous extract from the compactin producing fungal strain. *Process biochemistry*, 44(8): 939-943.
- Suriyakala, G.; Sathiyaraj, S.; Devanesan, S.; AlSalhi, M. S.; Rajasekar, A.; Maruthamuthu, M. K. and Babujanarthanam, R.** (2022). Phytosynthesis of silver nanoparticles from *Jatropha integerrima* Jacq. flower extract and their possible applications as antibacterial and antioxidant agent. *Saudi Journal of Biological Sciences*, 29(2): 680-688.
- Wady, A. F.; Machado, A. L.; Foggi, C. C.; Zamperini, C. A.; Zucolotto, V., Moffa, E. B. and Vergani, C. E.** (2014). Effect of a silver nanoparticles solution on *Staphylococcus aureus* and *Candida* spp. *Journal of Nanomaterials*, 2014: 1-7.
- Wahab, M.; Bhatti, A. and John, P.** (2022). Evaluation of antidiabetic activity of biogenic silver nanoparticles using *Thymus serpyllum* on Streptozotocin-Induced Diabetic BALB/c Mice. *Polymers*, 14(15): 3138.
- Wulandari, A. P.; Haifa, I. H.; Ratnaniati, D. and Rossiana, N.** (2021). Bactericidal activity of extracts and major fractions of endophyte metabolites of fungus *Cladosporium velox* against pneumonia and diarrhea pathogens. *AgBioForum*, 23(1): 84-91.
- Zhou, S.; Wang, M.; Feng, Q.; Lin, Y. and Zhao, H.** (2016). A study on biological activity of marine fungi from different habitats in coastal regions. *SpringerPlus*, 5(1): 1-8.